

Observations of the Ultra-Heavy Galactic Cosmic-Ray Abundances ($30 \leq Z \leq 40$) with TIGER

S. Geier^a, B.F. Rauch^b, L.M. Barbier^c, W.R. Binns^b, J.R. Cummings^c, G.A. de Nolfo^c, M.H. Israel^b, J.T. Link^b, R.A. Mewaldt^a, J.W. Mitchell^c, S.M. Schindler^a, L.M. Scott^b, E.C. Stone^a, R.E. Streitmatter^c and C.J. Waddington^d

(a) California Institute of Technology, Pasadena, CA 91125, USA

(b) Washington University, St. Louis, MO 63130, USA

(c) Goddard Space Flight Center, Code 661, Greenbelt, MD 20771, USA

(d) University of Minnesota, Minneapolis, MN 55455, USA

Presenter: Rauch, B.F. (brian@cosray.wustl.edu), usa-rauch-B-abs1-og11-oral

Observations of Ultra-Heavy galactic cosmic rays (GCR) help to distinguish the possible origins of GCRs. The Trans-Iron Galactic Element Recorder (TIGER) measures the charge (Z) and energy of GCRs using a combination of scintillation counters, Cherenkov counters, and a scintillating fiber hodoscope. TIGER has accumulated data on two successful flights from McMurdo, Antarctica: the first launched in December of 2001 with a total flight duration of 31.8 days and the second in December of 2003 with a total flight duration of 18 days. We present a preliminary analysis of the combined data from both flights for Ultra-Heavy GCRs.

1. Introduction and Scientific Motivation

The principal objective of TIGER is the determination of the source abundances of the heavy GCRs with $Z \leq 40$. These abundances can be used to address the questions surrounding the nature of the GCR source material and acceleration mechanism. Supernovae have long been thought to be responsible for accelerating the GCRs as they provide the power needed with a reasonable acceleration efficiency. There is evidence supporting the picture that the GCRs originate in superbubbles surrounding OB associations [1, 2], in which the source material arises from the outflows of Wolf-Rayet stars and from the ejecta of supernovae (SNII, SNIb,c) mixed with old interstellar gas. Two models have been proposed to explain the detailed composition of the GCR source material that is accelerated by supernova shocks. The first is based on the observation that GCR abundances are strongly enhanced over SS abundances based on first ionization potential (FIP) [3], which suggests that the GCR source might be an environment such as stellar atmospheres. The alternate model, based on volatility [4, 5], notes that most elements with low FIP also are refractory, which suggests that the GCR source could be enriched in material from interstellar dust grains.

TIGER data will improve the statistical precision for the elements ^{29}Cu , ^{30}Zn , ^{31}Ga , ^{32}Ge and ^{37}Rb , which break the FIP-volatility degeneracy. Previous measurements of UH (Ultra-Heavy $Z \geq 30$) GCRs were made by the HEAO-3 [6] and Ariel-6 [7] satellite instruments, which were able to resolve the even- Z elements in the $30 \leq Z \leq 60$ range but did not resolve the odd- Z elements. The HEAO-C2 experiment [8] provided a measurement for the lower part of this range but with limited statistics. Results from the 2001 TIGER flight [9] showed that the instrument has single charge resolution in the $30 \leq Z \leq 40$ range and yielded improved measurements of ^{30}Zn , ^{31}Ga and ^{32}Ge .

2. The TIGER Instrument

TIGER is a Long Duration Balloon (LDB) borne experiment capable of characterizing the charge and energy of the GCR with charges between $Z = 14$ (Silicon) and $Z = 40$ (Zirconium). The instrument, shown in Figure 1,

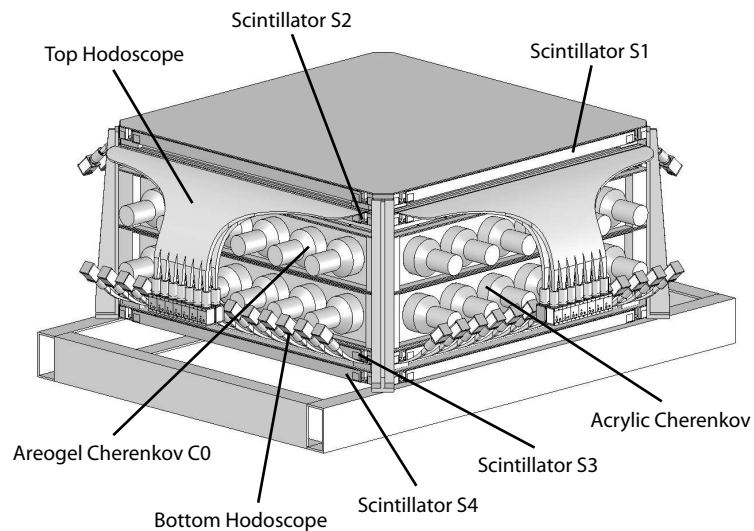


Figure 1. Side view of the TIGER instrument.

consists of four PVT scintillator radiators (St Gobains BC-416) read out with wavelength-shifter-bars (WLSB) (St Gobains BC-482A), two Cherenkov radiators in light collection boxes (one acrylic and one aerogel), and a scintillating optical fiber hodoscope. The radiators are arranged with two scintillators (S1 & S2) on top with a hodoscope plane (HT) in between. The two Cherenkov detectors are in the middle with the aerogel (C0) being above the acrylic (C1), and finally the other two scintillators (S3 & S4) with a hodoscope plane (HB) in between at the bottom. The light produced in the radiators and the hodoscope is measured using photomultiplier tubes (PMTs). The scintillators each have eight Hamamatsu R1924 PMTs mounted at the ends of the WLSBs that surround the radiator edges. The light collection boxes of the two Cherenkov radiators each have six Burle S83006F PMTs along each of their four edges. A total of 112 Hamamatsu R1924 PMTs are used in the two hodoscope planes. The signals from the PMTs are pulse height analyzed by the flight electronics.

The scintillators provide a measurement of light emitted as a function of path length traversed by the ionizing particle, dL/dx . The light produced is not directly proportional to the energy deposited due to saturation effects, which must be corrected for to determine the energy loss as a function of path length, dE/dx . The scintillators are also used in flight for the event trigger by requiring coincidence in top and bottom scintillators to ensure the particle is in the detector's geometry. In post flight analysis, the top and bottom scintillators are also used to eliminate events that may have interacted within the instrument.

The Cherenkov radiators measure the velocity of the incident particles and contribute to their charge measurement. Cherenkov radiation is produced by a particle traversing a medium with a velocity greater than the speed of light within that medium, and it is proportional to the square of the particle's charge (Z) and is a function of the particle's velocity. Two different Cherenkov radiators are used since their different indices of refraction, 1.5 for the acrylic and 1.04 for the aerogel, provide different energy thresholds, 0.32 and 2.5 GeV/nucleon respectively. Together, these radiators provide TIGER with energy sensitivity between 0.3 and 10 GeV/nucleon in the instrument.

The scintillating fiber hodoscope measures the trajectory of particles through the TIGER instrument. The hodoscope has two planes, each consisting of two layers of perpendicular fibers formatted into tabs of six 1 mm square fibers. The tabs are formatted to 14 PMTs at either end, with a fine side receiving every fourteenth

tab and a coarse side receiving groups of 14 consecutive tabs. This coding [10] allows for the determination of particle coordinates to within 6 mm for particles lighting only one tab and to within 3 mm for particles lighting more than one tab. The coordinates determined in the hodoscope layers are used to determine the angle of incidence of the particles and where they traverse the radiators. This allows corrections to be made for pathlengths and area effects within the radiators.

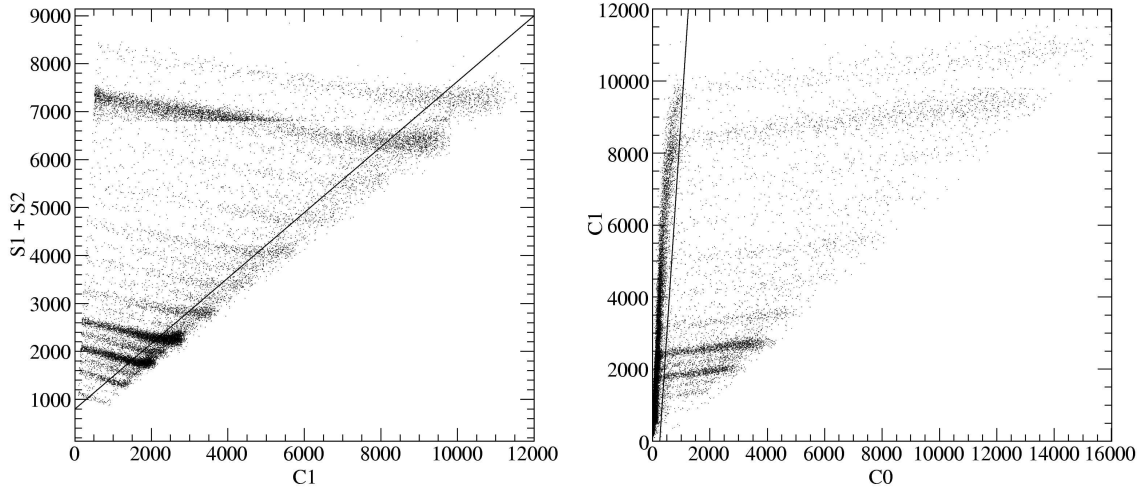


Figure 2. Crossplots of top scintillator signals versus acrylic Cherenkov signal (left) and acrylic Cherenkov signal vs aerogel Cherenkov signal (right) for the 2003 dataset with every 100th event below $S1 + S2 = 6800$ and every 10th above.

3. Results of Two Flights

TIGER has had two successful flights from McMurdo, Antarctica for a total of nearly 50 days. The December 21, 2001 - January 21, 2002 flight, lasting 31.8 days, had an average altitude of 118,800 ft (5.5 mbar). The altitude varied considerably over the duration of this flight from a high near 129,000 ft at the beginning to a low near 109,000 ft at the end due to a slow leak in the balloon. The December 17, 2003 - January 4, 2004 flight, lasting 18 days, had an average altitude 127,800 ft (4.1 mbar), with the altitude varying between a minimum of 121,000 and a maximum of 134,000 ft. There are $\sim 2/3$ as many high Z events from the 2003 flight as the 2001 due to the higher average altitude even though the flight was $\sim 1/2$ as long in duration.

Figure 2 shows crossplots for a sample of events from the 2003 dataset. The plot on the left shows the sum of the top scintillator signals ($S1 + S2$) plotted versus the sum of the acrylic Cherenkov signal ($C1$), which are used to determine Z for particle energies below the threshold of the aerogel Cherenkov ($C0$). We see that there is good separation between the charge contours for each element with the exception of the high energy nuclei to the right of the line showing the $C0$ threshold. There is a small relativistic rise in the scintillation signal which results in charge identification ambiguity in this energy region. The plot on the right shows the acrylic Cherenkov signal plotted versus the aerogel Cherenkov signal, which is used to assign charge (Z) to particles above the $C0$ threshold. The particles to the right of the line showing the $C0$ threshold, which show good charge resolution, are the particles to the right of the $C0$ threshold line in the left panel. Thus we have used $C0$ to resolve the ambiguity in charge assignment which results from a measurement of S and $C1$ only.

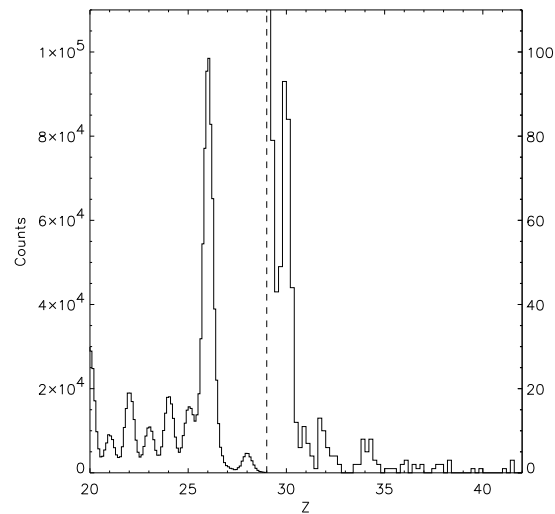


Figure 3. Charge histogram of combined dataset from 2001 and 2003 flights.

Our preliminary data from the 2003 flight is combined with our 2001 data in Figure 3. We see that the charge resolution is good and that clear peaks are observed for $Z = 30, 31, 32,$ and 34 . However, the analysis of the 2003 data is not sufficiently advanced to obtain elemental abundances.

4. Acknowledgments

This research was supported by the National Aeronautics and Space Administration under grant NNG05WC04G.

References

- [1] J.C. Higdon and R.E. Lingenfelter, *Ap.J.*, 590 (2003) 822.
- [2] W.R. Binns et al., 29th ICRC, India (2005) OG 1.
- [3] M. Casse and P. Goret, *Ap.J.*, 221 (1978) 860.
- [4] R.I. Epstein, *MNRAS*, 193 (1980) 723.
- [5] C.J. Cesarsky and J.P. Bibring, 1981, *Origin of Cosmic Rays*, IAU Symp. 94, ed. G. Setti, et al., 361.
- [6] W.R. Binns et al., *Ap.J.*, 346 (1989) 997.
- [7] P.H. Fowler et al., *Ap.J.*, 314 (1987) 739.
- [8] J.J. Engelmann et al., *A&A*, 233 (1990) 96.
- [9] J. Link et al., 28th ICRC, Japan (2003) OG 1, 1781.
- [10] D.J. Lawrence et al., *NIM-A*, 420 (1999) 402.